Journal of Materials Chemistry C

FEATURE ARTICLE

View Article Online
View Journal | View Issue

Published on 16 December 2013. Downloaded by University of Southern California on 06/10/2016 01:42:13.

Flexible photovoltaic technologies

Cite this: J. Mater. Chem. C, 2014, 2, 1233

Qingfeng Lin,[a] Hongtao Huang,[bc] Yan Jing,[d] Huiying Fu,[a] Paichun Chang,[e] Dongdong Li,*[b] Yan Yao*[df] and Zhiyong Fan*[a]

Received 7th November 2013
Accepted 16th December 2013

DOI: 10.1039/c3tc32197e

www.rsc.org/MaterialsC

Flexible photovoltaic (PV) devices have attracted enormous attention from academy and industry as a convenient alternative energy source for indoor and outdoor applications. Flexible PV panels can be easily integrated with infrastructures of various shapes and sizes, meanwhile they are light-weight and thus suitable for applications where weight is important. In this review, we will describe the progress that has been made in the field of flexible PV technologies. In addition, a summary will be provided with perspective on the future development of flexible solar cells and new opportunities offered by these devices.

1 Introduction

Electricity is the most extensively used form of energy, which is convenient to transport and store, and to convert to other forms of energy, such as mechanical energy, thermal energy, *etc.* However, it has been primarily produced by burning fossil fuels due to historical reasons. Unfortunately, the reserve of fossil fuels is limited and burning them is causing increasing environmental issues.[1–4] Therefore, exploring clean and renewable energy sources is becoming a pressing task to researchers all over the world.

Solar energy is one of the most abundant and renewable energy sources that is used in the world. Photovoltaic (PV) devices, which directly convert solar energy into electricity, have been regarded as promising candidates for a CO_2 emission free energy supply.[5] Indeed, installed solar PV capacity has increased rapidly from just 1 GW in 2000 to 67 GW in 2011, and is projected to be over 600 GW by 2035.[4]

Among various PV technologies, thin film PV is considered more cost-effective than traditional crystalline Si-based PV, which is not only more expensive, but also heavier and more fragile.[6] More importantly, the light-weight, mechanically

[a]Department of Electronic and Computer Engineering, The Hong Kong University of Science and Technology, Clear Water Bay, Kowloon, Hong Kong, China. E-mail: eezfan@ust.hk
[b]Shanghai Advanced Research Institute, Chinese Academy of Sciences, 99 Haike Road, Zhangjiang Hi-Tech Park, Pudong, Shanghai 201210, China
[c]Wuhan National Laboratory for Optoelectronics and College of Optoelectronic Science and Engineering, Huazhong University of Science and Technology, Wuhan, 430074, China
[d]Department of Electrical and Computer Engineering & Materials Engineering, University of Houston, Houston, TX 77204, USA
[e]Nano Ark Inc., San Jose, CA 95126, USA
[f]Texas Center for Superconductivity at UH, University of Houston, Houston, TX 77204, USA

Qingfeng Lin is a PhD candidate at the Department of Electronic and Computer Engineering in the Hong Kong University of Science and Technology. He received his BS degree in Electronic Science and Technology from the University of Science and Technology of China. His current research interests focus on the novel fabrication of three-dimensional nanostructures, and the applications of functional nanomaterials for energy harvesting, energy storage, and nanoelectronics.

Hongtao Huang is currently a joint PhD candidate of Huazhong University of Science and Technology and the Shanghai Advanced Research Institute, Chinese Academy of Sciences. His current scientific interests are optoelectronic thin film materials and devices.

Published on 16 December 2013. Downloaded by University of Southern California on 06/10/2016 01:42:13.

flexible thin film technologies open up new opportunities for PV device design, *i.e.* flexible solar cells, which offer a convenient alternative energy source for indoor and outdoor applications.[7–9] Flexible PV panels can be easily integrated with infrastructures of various shapes and sizes, consequently stimulating the design of innovative energy-generating products. Additionally, these flexible modules are light-weight and thus suitable for applications where weight is important, meanwhile they possess a much faster payback than conventional PV modules. Up-until-now, a lot of different PV materials have been developed with diverse deposition methods on a variety of flexible substrates to manufacture flexible solar cells. Accordingly, based on the PV materials used, flexible solar cells are usually categorized as (1) Si based flexible solar cells, (2) compound flexible solar cells, and (3) organic solar cells. In this review, we will describe the progress that has been made in the field of flexible solar cells. In addition, a summary will be provided with perspective on the future development of flexible solar cells and new opportunities offered by these devices.

2 Si based flexible solar cells

2.1 Flexible thin film c-Si solar cells

Among the various PV technologies, crystalline silicon (c-Si) solar cells hold the dominant market share due to the advantages of material abundance, broad spectral absorption range, high carrier mobilities, and its mature technology.[10] Wafer based solar cells have gained efficiencies as high as 24.7% in the research lab.[11] When the thickness decreases to <50 μm, a cell efficiency of 21.5% can still be obtained.[12] Meanwhile, further reducing the c-Si thickness down to a few micrometers can significantly reduce material usage and cost. Compared with bulk wafers, thin film c-Si solar cells have a potentially higher open circuit voltage (V_{oc}) and efficiency limits imposed by Auger recombination,[13] making thin film c-Si highly attractive for high performance flexible solar cells. However, the preparation of thin film c-Si still remains a challenge. The conventional wire saw technique used for wafer slicing creates large amounts of micron-size silicon powder "kerf".[14] As the wafer thickness (several tens micrometer) is much smaller than the wire

Yan Jing received his BS degree from the University of Science and Technology Beijing, China, in 2011. He then joined the University of Houston for his PhD degree under the supervision of Prof. Yan Yao in 2013. His research focuses on organic functional material design and synthesis for both organic solar cells and rechargeable lithium batteries.

Yan Yao received his PhD degree from the University of California, Los Angeles in 2008. From 2008 to 2010, he worked at Polyera Corporation as a senior scientist. From 2010 to 2012, he then worked at Stanford University as a postdoctoral fellow. In September 2012, he joined the University of Houston as an Assistant Professor. He has published more than 30 peer-reviewed papers with 7000+ citations. He holds 1 US patent and 8 patent applications. His research effort concentrates on nanostructured materials and devices for energy storage and conversion.

Dongdong Li received his PhD degree in Materials Science from Shanghai Jiao Tong University in 2010. Under the support of the Ministry of Education of the People's Republic of China, he worked in the Department of Electrical Engineering at the University of Southern California (2007–2009). Currently, he is an associate professor at the Shanghai Advanced Research Institute, Chinese Academy of Sciences. His research focuses on the structural and interfacial engineering of functional nanomaterials, for technological applications in energy conversion and storage.

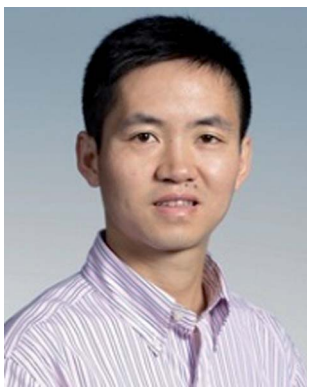

Zhiyong Fan received his PhD degree from the University of California, Irvine, in 2006 in Materials Science. From 2007 to 2010 he worked at the University of California, Berkeley, as a postdoctoral fellow in the department of Electrical Engineering and Computer Sciences, with a joint appointment with Lawrence Berkeley National Laboratory. In May 2010, he joined the Hong Kong University of Science and Technology as an assistant professor. His research interests include engineering novel nanostructures with functional materials for technological applications including energy conservation, electronics and sensors, etc.

This journal is © The Royal Society of Chemistry 2014

Published on 16 December 2013. Downloaded by University of Southern California on 06/10/2016 01:42:13.

diameter (150–200 μm), the kerf loss as a fraction of the total ingot will be dramatically increased. In order to develop low-cost flexible PVs, several methods have been investigated to fabricate c-Si thin film and solar cells.

2.1.1 Epitaxial growth and layer transfer. One of the most famous approaches is the so-called ELTRAN (Epitaxial Layer TRANsfer) process which enables a high quality monocrystalline silicon thin film on foreign substrates.[15] The process sequence starts with the epitaxial growth of monocrystalline silicon thin film on silicon wafer with a separation layer. After device fabrication, the silicon thin film is bonded to a foreign substrate, and detached from the wafer. In this way, the starting wafer can be reused for another process cycle, rendering a reduction of materials waste. The growth of silicon thin film can be conducted using either liquid phase epitaxy (LPE)[16] or chemical vapour deposition (CVD).[17] The key step of the ELTRAN process is the fabrication of a separation layer.

Porous silicon (PS) is the most popular choice, which allows both the growth and separation of high quality epilayers. The PS is formed by the anodic dissolution of silicon wafer in HF solutions.[18] The porosity can be controlled by varying either the current density or HF concentration. Typically, a bi-layered PS with a high porosity (50–70%) layer beneath a low porosity (10–20%) layer is required for the growth and transfer process.[17] A high temperature treatment (>1050 °C) in a H_2 atmosphere induces a restructurization process in the PS, driven by the lowering of the free surface energy.[19] As a result, the low-porosity layer forms a quasi-monocrystalline silicon (QMS) film with enclosed voids several tens of nanometers in diameter, serving as the seeding layer for epitaxial growth. Meanwhile, large voids with a lateral extension of several tens of micrometers are formed in the high-porosity layer. The remaining few bridging silicon allow the epilayer to be detached from the substrate wafer (Fig. 1a).

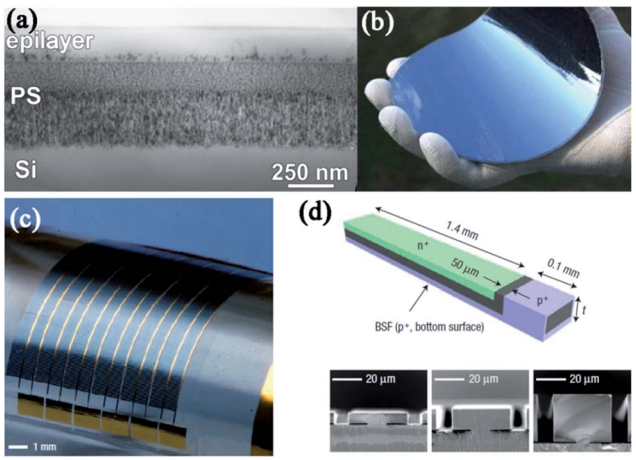

Fig. 1 (a) Epitaxial grown silicon thin film on bi-layered PS. Reprinted from ref. 17. (b) 150 mm flexible c-Si solar cell based on porous silicon. Reprinted from ref. 20. (c) Flexible c-Si solar cell modules fabricated by an undercut etching of bulk silicon. (d) SEM image of the microbar after undercut etching and schematic illustration of an individual microcell. Reprinted from ref. 22.

After *in situ* device fabrication, the device is mounted to a transparent flexible polymer foil and detached from the host wafer directly by mechanical force. The whole fabrication process is ended by the evaporation of Al back contact. Following this process, Werner and co-workers successfully demonstrated flexible c-Si solar cells with 150 mm diameter sandwiched in two plastic sheets (Fig. 1b).[7,20] Taking advantage of the high quality monocrystalline characteristics, an efficiency up to 14.6% was achieved in 2006.[20] Recently, based on PS, Solexel announced 156 × 156 mm^2 square flexible c-Si solar cell products with a record efficiency as high as 20.1% in 2012.[21]

2.1.2 Etch-release method. In addition to the epitaxial growth of c-Si thin film, the mature micro-fabrication techniques from the semiconductor industry also provide alternative strategies for the flexible thin film c-Si solar cells. As shown in Fig. 1c and d, Yoon *et al.* demonstrated ultrathin monocrystalline silicon flexible PV modules composed of well organised interconnected microbar solar cells.[22] These microbars are fabricated through the anisotropic undercut etching of silicon wafers. As shown in the SEM images of Fig. 1d, the undercut etching facilitates the release of microbars from the wafer with narrow anchors. In order to complete the microcell fabrication, the p–n junction, top contacts and back-surface field are created by selective-area diffusion, as shown in the schematic illustration of Fig. 1d. A soft and elastomeric stamp, usually polydimethylsiloxane (PDMS), is used to retrieve these microcells from the wafer and print them onto a flexible polymer substrate. The interconnection of microcells can be obtained through metal evaporation or direct conductive ink printing. The individual microcells of 15–20 μm thickness show efficiencies in the range of 6–8%, which can be increased to 10–13% with back reflectors. The efficiency of the flexible module remains unchanged at a bending radius of 4.9 mm and only shows little degradation with bending up to 200 cycles, indicating good mechanical robustness for flexible applications.

A similar approach has been developed by Cruz-Campa *et al.* to fabricate flexible PV modules composed of hexagonal silicon segments (14 μm in thickness) with an efficiency of 14.9%.[23]

2.1.3 Exfoliating from bulk silicon wafer. Besides the above-mentioned strategies, a much simpler exfoliation method has been demonstrated recently.[24–26] A Ni film is first deposited by sputtering[24] or electroplating[25,26] as the stressor layer with controlled thickness and stress. Then a flexible handle layer is attached to the stressor, which prevents multiple fractures and the cracks formed during spalling.[24] Initiated by a pre-determined crack, the silicon thin film is finally exfoliated. IBM demonstrated flexible solar cells with efficiencies of 4.3% on monocrystalline silicon foils prepared by the controlled spalling.[24] The major factor causing this low efficiency is the thin thickness of the silicon foil (~3 μm) that cannot absorb light sufficiently. The thickness of the exfoliated layer can be controlled by varying the metal thickness, deposition conditions and the pre-determined crack parameters. With controlled conditions, Saha *et al.*,[26] reported a thicker (~25 μm) silicon foil which enables a double side texturing process and promising performances with a short circuit current density (J_{sc}) and efficiency up to 34.4 mA cm^{-2} and 14.9% respectively.

Published on 16 December 2013. Downloaded by University of Southern California on 06/10/2016 01:42:13.

Note that all the above-mentioned approaches can be classified into three subdivisions: preparation of the Si active layer, transfer of the silicon thin film, and fabrication of devices. The device fabrication can be conducted either before or after the layer transfer process. However, the preferred sequence is that most of the fabrication process should be performed before the transfer, concerning the high temperature issue.[20] Besides the active layer preparation and substrate materials, the flexible solar cell fabrication process is similar to the conventional wafer based solar cells that includes the doping of the back-surface field, diffusion of the selective emitter, deposition of passivation, anti-reflection layer and the contacts.

2.2 Flexible thin film a-Si:H/μc-Si:H solar cells

Compared with flexible c-Si solar cells, hydrogenated amorphous (a-Si:H)/microcrystalline (μc-Si:H) silicon thin film solar cells have the advantages of better weak light performance, large scale production under a lower temperature and superior flexibility, which is quite suitable for the large scale deployment of low-cost PVs on a flexible substrate.

2.2.1 Materials and facilities. The active layer of a-Si:H/μc-Si:H single junction solar cell is a stack (~300 nm or several micrometers thick) composed of three silicon layers, *i.e.* the n- and p-type doped layers and an intrinsic (i-) layer between them. The n- and p-layers create a rectifier diode, while the i-layer absorbs the most incident light.

The silicon films are generally obtained in a plasma-enhanced chemical vapour deposition (PECVD) system using H_2 diluted SiH_4 as the source precursor while PH_3 and B_2H_6 are the n- and p-type dopant sources. Other techniques, such as hot wire CVD (HWCVD),[27] inductively coupled plasma CVD (ICPCVD),[28] and very high frequency PECVD (VHF-PECVD),[29] are also being investigated for high quality or high-throughput solar cell manufacturing. The crystal phase of Si:H can be controlled by the H_2-to-Si:H_4 dilution ratio (R) and the film thickness (d_b).[30] When increasing R or d_b, a transition starting from the amorphous growth region, to the mixed phase (amorphous and microcrystalline) growth region, and finally the pure microcrystalline growth region can be observed (Fig. 2a). This phase diagram provides a guideline for the optimization of active materials and the cell performance.

Although single-chamber processes for a-Si:H solar cell deposition have been utilized to lower the equipment cost, cascade (Fig. 2b) or cluster deposition systems with multiple chambers for different layers are preferable to avoid contamination from doped layers to i-layers. In the case of mass production, flexible a-Si:H and μc-Si:H solar cells are preferred to be fabricated through a roll-to-roll production line. As shown in Fig. 2c, the roll-to-roll system contains not only the PECVD chambers for the deposition of active layers, but also the processes to fabricate the whole solar cells, including cleaning of the substrates, connecting hole punching, sputtering, laser scribing, printing of top contacts, evaluation, and encapsulation.[31,32]

In practice, tandem cells and triple-junction cells have been extensively investigated and are used for most commercial

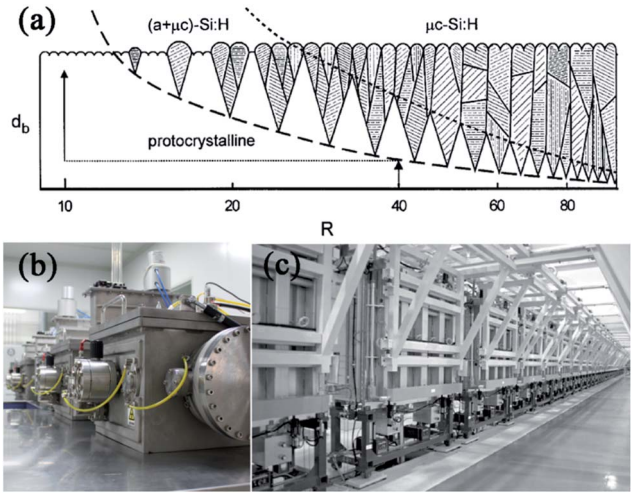

Fig. 2 (a) Schematic of the structure of Si:H films as a function of R and d_b. Reprinted from ref. 30. Photographs of (b) a research cascade deposition system at the Shanghai Advanced Research Institute, Chinese Academy of Sciences, and (c) United Solar's 30 MW continuous roll-to-roll Ovonic a-Si PECVD processor. Reprinted from ref. 31.

modules, aiming at increasing the performance by maximizing the full solar spectrum absorption.[33–35] The bandgaps of a-Si:H and μc-Si:H in the multi-junction devices are tuned to ~1.7 eV and ~1.1 eV for blue and infrared spectrum absorption respectively.[35] Amorphous silicon-germanium alloy (a-SiGe:H) is an additional material choice for absorbing the green and red photons, with a tunable bandgap through controlling the silicon-to-germanium ratio.[8] Different configurations of tandem and multi-junction solar cells have been demonstrated based on these materials, such as a-Si:H/a-Si:H tandem cell,[33] a-Si:H/μc-Si:H tandem cell[36] and a-Si:H/a-SiGe:H/a-SiGe:H triple-junction cell.[8]

2.2.2 Device structure configuration. Two different configurations, *i.e.* "superstrate" and "substrate", have evolved in PV device design based on the starting materials in the fabrication process.[37] In the "superstrate" design, incident light will have to pass through the transparent substrate before entering absorbing layers. However, most transparent plastics will suffer serious deformation under the general processing temperature (~300 °C). Thus "substrate" design, configured as an n–i–p structure, is generally accommodated in flexible a-Si:H solar cells, using metal or opaque plastic foils with good temperature tolerance. Stainless steel is the most popular choice owing to the advantages of low cost, high mechanical strength and ease of preparation.[8,38,39] For example, United Solar (Uni-Solar), a US PV manufacturer, demonstrated triple-junction amorphous silicon alloy solar cells on stainless steel (Fig. 3a) with an initial efficiency of 14.6% and a stable efficiency of 13% in 1997.[8,40]

Due to the characteristic of being light weight, plastic substrates possess unique advantages for applications like aerospace and wearable PV devices. Some heat-resisting plastic films like polyimide (PI) can endure the elevated temperature during PECVD and sputtering processes to deposit silicon thin film solar cells, as shown in Fig. 3b.[41] Although the mechanical strength and thermal stability of polymers are not comparable

This journal is © The Royal Society of Chemistry 2014

Published on 16 December 2013. Downloaded by University of Southern California on 06/10/2016 01:42:13.

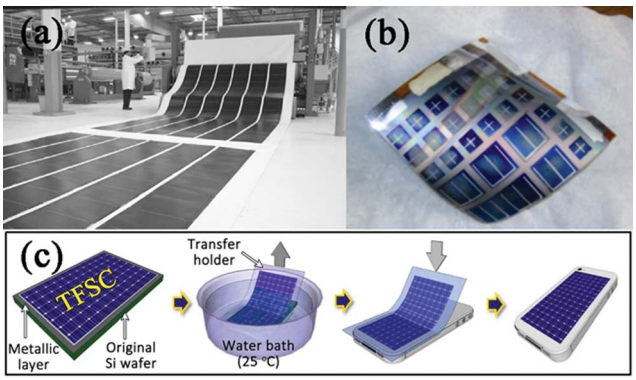

Fig. 3 (a) Roll of laminate roofing product integrating Unites Solar Ovonic triple junction a-Si on stainless steel with a membrane at Solar Integration Technology's plant in CA, USA. Reprinted from ref. 40. (b) Triple junction a-Si cells on Mo-coated Kapton VN. Reprinted from ref. 41. (c) Schematic of the peel–stick process. Reprinted from ref. 45.

with that of metal foils, high efficiency devices have also been realized.[32,42,43] Fuji Electric developed a-Si:H/a-SiGe:H based tandem solar cells on plastic substrate and achieved a stabilized efficiency of 9% in a 40 cm × 80 cm cell.[32] The fabrication of this flexible solar cell was conducted in roll-to-roll apparatuses. Similarly, Uni-Solar demonstrated triple-junction ultra-light-weight a-Si:H/a-SiGe:H/a-SiGe:H solar cells on ~25 μm plastic substrate using roll-to-roll deposition. This material gives an initial aperture-area efficiency of 9.84% and specific power of ~1200 W kg^{-1}.[44]

In addition to searching for suitable heat-resisting polymers as substrate materials, the advanced design of the processing sequence can also allow the fabrication of flexible solar cells on plastics. As shown in Fig. 3c, Lee *et al.* developed a peel-and-stick method to construct a thin film solar cell on universal substrates without changing the material deposition conditions and performance.[45] This was realized by separating the attachment of solar cell onto the substrate from the material deposition process. The solar cells were first fabricated using conventional parameters on nickel coated Si wafer rather than the plastic. Then the solar cell was coated with a polymer and attached to a thermal release tape as a temporary holder and soaked in a water bath at room temperature. Water-assisted subcritical debonding separates the device from the wafer, leading to the free-standing solar cell on polymer substrates. After releasing the tape, ultrathin flexible solar cells are obtained which can be transferred and attached to universal substrates.

2.3 Efficient light management for Si thin film solar cells

As described above, flexible Si based PV devices usually consist of a rather thin active layer. Therefore, efficient light absorption in such thin film flexible Si based solar cells is essential for enhancing energy conversion efficiency and lessening cost, which requires a broadband antireflection effect and efficient light trapping mechanism.[46,47] A variety of nanostructures with photonic materials have demonstrated a promising capability of capturing the incident photons over a broad range of wavelengths and incident angles.[48–52]

In this regard, Wang *et al.* recently demonstrated a large-area free-standing ultrathin single-crystalline Si at the wafer scale as a new Si material for the fabrication of double-sided nanocone solar cells.[53] The ultrathin single-crystalline Si was fabricated by KOH etching the Si wafer to a uniform thickness from 10 μm to thinner than 2 μm. These ultrathin Si films exhibit excellent mechanical flexibility and bendability, as demonstrated in Fig. 4a, a 3 μm thick Si film wrapped around a rod with diameter of 7 mm. Furthermore, double-side nanotextures were patterned on the free-standing ultrathin Si films for efficient light absorption, as illustrated in Fig. 4b. It was demonstrated that the top-side texturing enhanced the photocurrent largely due to the antireflection effect caused by the gradual effective refractive index, while the back-side patterning increased the photocurrent further by the light scattering effect. Following the nanotexturing processing, a 6.8 μm thick front-side nanotextured solar cell with a power conversion efficiency of 6.2% was fabricated without supporting substrates, which opens up new possibilities for flexible single-crystalline Si PV devices.

On the other hand, in the substrate configuration of flexible thin film a-Si:H/μc-Si:H solar cells, the metal or plastic foils generally have flat surfaces without well designed light trapping textures. There have been few available strategies to directly fabricate textured structures for efficient light management on flexible substrates before, except for depositing textured TCO layers. Recently, Li and co-workers demonstrated a-Si:H thin film solar cell with enhanced light absorption and performance on low-cost nanodent array aluminium foils, as shown in Fig. 4c and d.[54] Prepared by a facile electrochemical anodization of

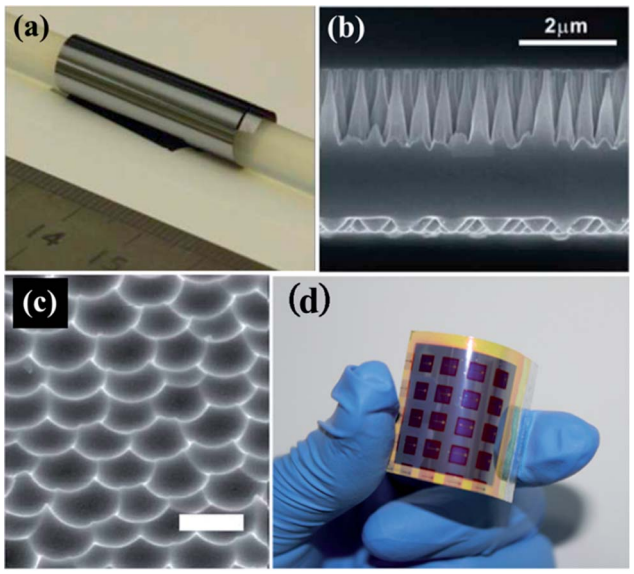

Fig. 4 (a) Photograph of a 3 μm thick Si film wrapped around a plastic rod with a diameter of 7 mm. (b) Cross-sectional SEM image of a double-sided nanotextured Si film. Reprinted from ref. 53. (c) SEM image of a nanodent array on an aluminium substrate. (d) a-Si:H solar cells on a nanodent array alumina substrate. Reprinted from ref. 54.

Published on 16 December 2013. Downloaded by University of Southern California on 06/10/2016 01:42:13.

aluminium, this light trapping structure allows efficient scattering and the excitation of waveguide modes, surface plasmon polaritons (SPPs) and localized surface plasmon resonances (LSPs). The J_{sc} and efficiency were improved by 31% and 27% respectively. In conjunction with a roll-to-roll anodization process,[55] this novel substrate holds attractive potential to be integrated with the present roll-to-roll fabrication system of flexible solar cells.

3 Flexible compound solar cells

Besides c-Si, a-Si:H and μc-Si:H, crystalline compound semiconductor materials, such as CdTe, Cu (In,Ga)Se_2 (CIGS), and III–V semiconductors have also been intensively studied for low-cost PV modules with high efficiency and excellent stability. The deposition of compound semiconductors onto flexible substrates initiates new fields of solar cell applications, as well as enabling the implementation of roll-to-roll deposition methods and the monolithic integration of solar cells. For example, the demonstration of a CIGS solar cell grown on flexible polyimide film with a power conversion efficiency of 18.7% revealed that flexible solar cells with a performance comparable to those on rigid substrates can be achieved.[56] A recent innovation of the precise controlling over the amount of copper atoms penetrating into the CdTe layer boosted a power conversion efficiency of 11.5% for a CdS/CdTe solar cell based on a flexible molybdenum foil substrate.[57] On the other hand, single crystalline III–V compound solar cells with power conversion efficiencies over 30%, which consist of lattice-matched epitaxial layers grown on a Ge or GaAs substrate, have already been put to practical use in power generators for space satellites. Recent demonstration of a conversion efficiency of 44.4% for GaAs multi-junction solar cells in Sharp makes these solar cells the best candidate for terrestrial concentrator PV systems (Sharp, 2013). Research in advanced materials and mechanics has uncovered ways to build mechanically flexible and even stretchable GaAs solar cell systems, due to decades of tremendous efforts in PV technology.[58,59] In the following sections, flexible solar cells made of CdTe, CIGS and GaAs will be introduced as they are relatively mature material systems. Meanwhile, it is worth pointing out that even though CdTe and GaAs have been heavily used for thin film PVs, their toxicity has become a rising concern, in this regard, earth abundant and environmental friendly PV materials such as copper–zinc–tin–selenide (CZTS) have also been actively explored.[60–63]

3.1 Flexible CdTe solar cells

Up-until-now, CdTe has been one of the leading thin film PV materials due to its optimum band-gap of 1.5 eV for efficient PV conversion. High efficiency, decent stability, and most importantly, low dollar per watt cost of CdTe solar cells make CdTe an attractive active material. The present status of the thin film CdTe solar cells is 19.6% efficiency for lab scale devices on transparent conductive oxide (TCO) coated glass superstrates (GE, 2013), 13.8% efficiency for devices on flexible polymer sheet substrates (Swiss Federal Laboratories for Materials Science and Technology (EMPA) and DuPont, 2011), and 11.5% efficiency for devices on flexible metallic foil substrates.[57] The industrialization of the CdTe PV technology has pushed the efficiency of the CdTe PV module efficiency to 16.1% (first solar, 2013).

3.1.1 Substrate configuration. In conventional CdTe solar cells based on TCO glass superstrates, glass takes up 98% of the device thickness and weight. Glass is known to be rigid and brittle, which requires extra care and substantial support for fabrication and installation. However, the weight and mechanical issues with glass can be eliminated by the utilization of flexible substrates, such as metallic foils or polymer sheets. Starting from the 1990s, attempts have been made to develop CdTe solar cells on metallic molybdenum foils in a substrate configuration where a power conversion efficiency of 5.3% were reported with the thermally evaporated CdTe absorber layer.[64] With magnetron sputtering used for the deposition of CdTe and CdS and an interlayer of ZnTe:N employed between CdTe and the back contact, an efficiency of 7.8% was demonstrated for CdTe solar cells on molybdenum substrates.[65] The barriers in the development of CdTe devices on metallic substrates are factors including the mismatching of thermal expansion coefficients, diffusion of impurities during $CdCl_2$ annealing, and difficulties to form efficient ohmic back contact between CdTe and metallic substrates.

Thereafter, considerable effort, such as introducing telluride as the back contact for the CdTe solar cell, immersing the CdTe device in a $CuCl_2$ solution to obtain Cu-doping for CdTe, and preparing ZnTe:Cu or ZnTe as the interlayer between CdTe and the back contact Mo to facilitate the formation of an ohmic contact to CdTe, has been spared to improve the performance of flexible CdTe solar cells based on metallic substrates.[66–68] However, the efficiencies of CdTe solar cells fabricated on flexible metallic substrates have stayed below 8% for the last ten years until the recently reported 11.5% for a CdTe cell based on a Mo substrate.[57,69–71] The reason for the achievement of the breakthrough efficiency of 11.5% for CdTe cells on Mo substrates was the precisely controlled Cu doping of the CdTe layer.[57] It was demonstrated that adding 0.8×10^{15} Cu atoms per cm^2 to a 5 μm thick CdTe layer resulted in an abrupt decrease in resistivity by three orders of magnitude and an increase in hole density from less than 10^{12} cm^{-3} to 3.8 (± 0.6) $\times 10^{14}$ cm^{-3} as determined by Hall effect measurement. By performing electron beam-induced current (EBIC) measurement, the depth-dependent collection efficiency of solar cells with and without Cu doping showed that the efficiently collected carriers were those generated close to the electrical back contact, while the effective carrier collection for Cu-doped CdTe cells happened in a region close to the CdS layer (Fig. 5a and b). Based on this unique feature, over 90% of the usable sunlight is absorbed in the first micrometer of the CdTe layer near the CdS layer, Cu doping shifts the region of the effective collection of carriers to the region of carrier generation, which leads to a dramatic increase in the efficiency. As confirmed with capacitance–voltage measurements,

 This journal is © The Royal Society of Chemistry 2014

Published on 16 December 2013. Downloaded by University of Southern California on 06/10/2016 01:42:13.

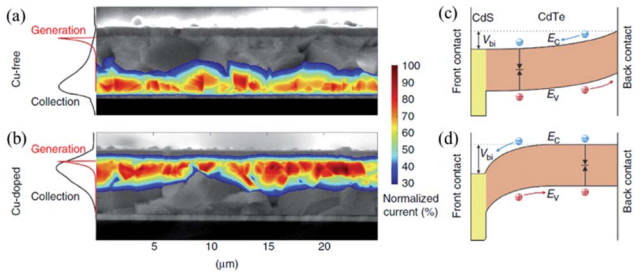

Fig. 5 EBIC measurements of CdTe solar cells processed (a) without Cu and (b) with 1×10^{15} Cu atoms per cm^2. Proposed energy band diagrams for CdTe solar cells (c) without and with (d) optimum Cu doping. Reprinted from ref. 57.

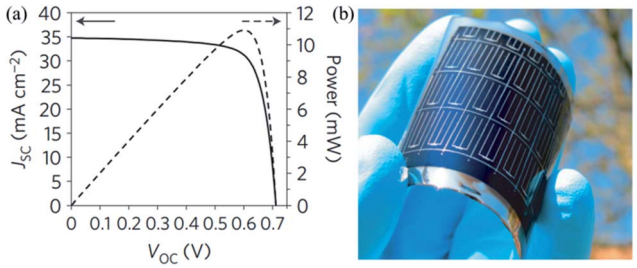

Fig. 6 (a) Current density–voltage (J–V) and power-voltage measurement curves of the certified 18.7% efficiency CIGS device. (b) Photograph of CIGS solar cells on a polyimide film. Reprinted from ref. 56.

the Cu-doped CdTe cell had a space charge region of about 1.8 μm (about 5 μm for Cu-free CdTe cell) which led to the effective carrier collection caused by sufficient band bending close to the CdS layer to generate a strong electric field (Fig. 5c and d).

3.1.2 Superstrate configuration. On the other hand, flexible CdTe/CdS solar cells have been developed on polyimide films in a superstrate configuration where the cells are grown on TCO-coated polyimide substrates. Solar cells of 8.6% efficiency were reported on ZnO:Al-coated in-house built polyimide film with a 'lift-off' method in 2001.[72] Later on, the efficiency for CdTe cells on polyimide substrates was further increased to 11.3% by utilizing indium tin oxide (ITO) as the front contacts for the cells.[73] By using commercially available thin polyimide (Unipex™) foils as the substrate, solar cells with an efficiency of 11.4% were presented.[74] The development of coating polyimide film with Al doped ZnO as the front electrical contact and highly transparent and resistive ZnO as the buffer layer led to the achievement of 12.4% efficiency for flexible CdTe cells in 2009.[75] To date, the highest reported efficiency for flexible CdTe cells with superstrate configuration on polyimide substrates is 13.8%.[76] Higher efficiencies for flexible CdTe cells are anticipated, while tremendous efforts are being made towards the back contact improvement and doping control of flexible CdTe solar cells.

3.2 Flexible CIGS solar cells

Cu (In,Ga)Se_2, also known as CIGS, is cadmium-free which is a more environmentally friendly material for thin film solar cells. The solar cells fabricated with polycrystalline CIGS as the absorber layer have yielded the highest power conversion efficiency of 20.4% among the thin film solar cell technologies [EMPA, 2013]. Meanwhile, CIGS thin film solar cells are of interest for space power applications because of the near optimum bandgap for AM0 solar radiation spectrum in space. Development of lightweight flexible CIGS solar cells deposited on flexible stainless steel (SS) foils or polyimide films have the potential for achieving high specific power. Up to date, the highest flexible cell efficiency of 18.7% for CIGS cells has been demonstrated on a polyimide film (Fig. 6).[56]

3.2.1 Mo, Ti, Al substrates. For flexible CIGS PV devices, various substrate materials, such as Mo, Ti, stainless steel, enameled mild steel and Al foils, flexible zirconia sheets, polyimide films and polyethylene terephthalate (PET) sheets have been studied.[77–84] The first demonstration of flexible CIGS solar cells on Mo substrates was reported with an efficiency of 8.3% by International Solar Electronic Technology back in 1993.[77] After years of research work, the Institute for Advanced Industrial Science and Technology (AIST, Japan) was capable of fabricating flexible CIGS cells on Mo foil with efficiencies above 14% in 2010.[85] An efficiency of 12% for flexible CIGS cells on Ti foil was demonstrated in 2000.[78] Later, Hahn-Meitner-Institut (HMI, Germany) reported an improved value of 15% for flexible CIGS cells on Ti foil without anti-reflection coating and a value of 17.4% with anti-reflection coating.[86,87] In 2009, an efficiency as high as 17.9% was reported for flexible CIGS cells on Ti foil by deploying a three state coevaporation of CIGS deposition and a ZnS(O,OH) buffer layer.[88] By depositing alkali-silicate glass thin film onto Ti foil, an efficiency of 17.4% was demonstrated for flexible CIGS cells.[79,89] Al foils have also been studied as flexible substrates for CIGS solar cells and the highest efficiency value of 17.1% was obtained (Nanosolar, 2011).

3.2.2 Steel substrates. Steel foil is a promising substrate for flexible CIGS solar cells because of its stability at the high temperatures involved during CIGS processing and the commercial availability. The highest efficiency of 17.7% for flexible CIGS cells on stainless steel was reported in 2012.[90] Compared to stainless steel, mild steel as a flexible substrate can introduce impurity diffusion in the CIGS layer. By depositing enamel layers as the insulating layer onto mild steel foil, a power conversion efficiency of 17.6% (certified) was obtained.[81]

3.2.3 Polymer substrates. The development of high efficiency flexible solar cells based on polymer substrates is limited by the requirement of low CIGS deposition temperatures restricted by the thermal–physical properties of polymers (polyimide as the generally used material). CIGS layers with suitable structural and optoelectronic properties should be deposited at temperatures lower than 500 °C as polyimides have the tendency to degrade at higher temperatures. The first report of flexible CIGS solar cells on polyimides showed an efficiency of

Published on 16 December 2013. Downloaded by University of Southern California on 06/10/2016 01:42:13.

8.7% achieved by a two-step process of sputtering metal precursors followed by a selenization reaction in 1996.[82] A significant improvement was achieved in 1999 with an efficiency of 12.8% by coevaporation of the CIGS layer on a spin-coated polyimide film atop NaCl/glass, followed by a lift-off after the solar cell fabrication.[83] Moreover, optimization of the buffer, window, grid and antireflection layers to reduce the optical and electronic losses resulted in the improved efficiency from 13.2% in 2004 to 16% in 2009 and 17% in 2011.[91–93]

3.2.4 Mini-module production. Furthermore, mini-modules and a large-area scale-up of flexible CIGS solar cells has also been developed on different substrates. Mini-modules with energy conversion efficiencies of 15.0% on enameled mild steel and 15.9% on zirconia sheets have been reported by using monolithic integration.[81,94] Furthermore, a monolithically integrated mini-module with an efficiency of 14.8% has been fabricated on polyimide substrate with a CIGS layer grown at EMPA and laser patterning done by the company Flisom AG.[92] Further development and optimization could lead to 20% efficiency flexible solar cells based on polyimide substrates, close to that based on rigid glass substrates.[56,95]

3.3 Flexible GaAs solar cells

3.3.1 Thin film GaAs PV cell technology. Crystalline GaAs has been used as a highly efficient absorbing layer in PV devices, GaAs solar cells with efficiencies above 25% were reported at 1-sun concentration and air mass 1.5 global (AM1.5G) and 1-sun AM0 back in the 1990s.[96] Besides the high efficiency, GaAs compound materials have advantages, including high photon absorption by the direct band gap energies, higher resistivity against high-energy rays in space, and smaller heat degradation compared with Si solar cells. GaAs solar cells made by the method of epitaxial lift-off (ELO) make it possible to remove the underlying GaAs or Ge substrates and place the thin film solar cells on the top of any other lower band gap solar cells or transfer the thin film solar cell to new support substrates that are thin, flexible and lightweight.[97–99] ELO of GaAs yields the highest reported efficiency of 28.8% post lift-off, which shows the negligible effect of the transferring technique on cell operation (Alta Devices, 2013).[100,101] Enhanced efficiencies can be realized by stacking GaAs cells either monolithically or mechanically on booster cells or lower band gap materials, such as CIS, Si, Ge, InGaAs, *etc*. A world record-setting efficiency of 37.9% at AM1.5G has been demonstrated for an InGaP (1.88 eV)/GaAs/InGaAs (0.97 eV) triple-junction solar cell fabricated using the inverted layer transfer process (Sharp, 2013).[102,103] The inverted epistructures make it possible to grow the lattice-matched and lattice-mismatched subcells in one growth run on one side of the parent substrate and in the proper optical sequence.

3.3.2 Flexible GaAs solar cells. Specifically for the space application, lightweight, thin and flexible GaAs solar cells have been developed. Paper-like InGaP/GaAs solar cells with an efficiency of 29.4% on flexible metal film was first reported by Sharp Corp. in 2005.[104,105] Later in 2006, Sharp discussed the application of flexible InGaP/GaAs cells for space solar panel and a prototype unit panel using laminated cells was developed for space application.[106] In the same year, Spectrolab Inc., a subsidiary of Boeing, reported a demonstration of a large-area (26.6 cm^2) and ultra-thin (less than 10 μm) InGaP/GaAs solar cells with an efficiency of 21%.[107] The first flight demonstration of film laminated InGaP/GaAs solar cells was presented by Japan Aerospace Exploration Agency (JAXA) in 2012.[108] The main feature of the mounted cells was that they were laminated with a transparent polymer film in place of the coverglass to take advantage of their flexibility and lightweight.

3.3.3 Module fabrication. For single-junction GaAs solar cells, Alta Devices reported a module efficiency record of 23.5% under AM1.5G at one sun illumination.[109] Research on flexible GaAs modules has demonstrated the integration of thin film GaAs solar cells with soft, elastomeric substrates to yield systems with linear elastic mechanical responses to strains. A flexible GaAs multijunction solar blanket with a three- and twelve-cell coupon with a coupon efficiency of 28% under AM0 conditions was reported by Spectrolab in 2006.[110] GaAs single-junction cells on PET (50 μm) based flexible modules showed a capability of bending to a radii of curvature of less than 5 mm without degradation in performance.[111] Moreover, stretchable solar modules with single-junction and multijunction GaAs solar cells was demonstrated.[58,59] In 2012, MicroLink Devices reported the flexible solar sheets consisting of arrays of interconnected large-area ELO GaAs solar cells with an efficiency of 29%.[112] A novel layer transfer technique called controlled spalling was developed and employed in the fabrication of ultralight flexible dual-junction GaAs solar cells on plastic (Fig. 7).[24,113] The bending endurance of the flexible GaAs cell was successfully demonstrated up to 1000 cycles at a radius of 10 mm without any noticeable change in device characteristics.

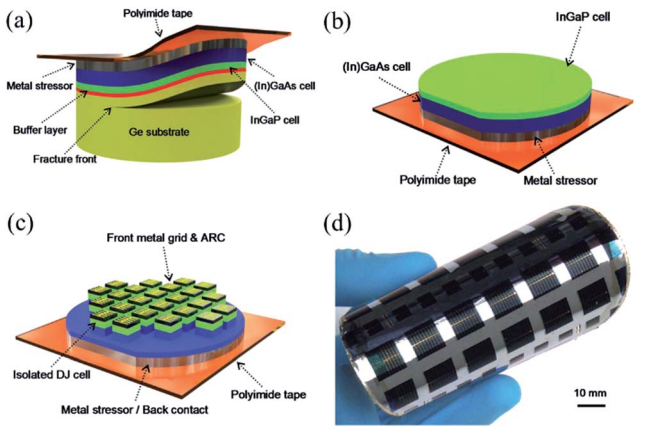

Fig. 7 Schematic diagram of the key processes for fabricating the flexible III–IV solar cells involving (a) controlled spalling to separate the solar cell structure from the growth wafer, (b) selective removal of the excess Ge and the buffer layer to expose the solar cell structure, (c) front grid and ARC deposition and cell isolatoin. (d) Photograph of the final 100 mm diameter flexible InGaP/(In)GaAs tandem solar cell on plastic. Reprinted from ref. 113.

This journal is © The Royal Society of Chemistry 2014

Published on 16 December 2013. Downloaded by University of Southern California on 06/10/2016 01:42:13.

4 Flexible and stretchable organic solar cells

The flexibility and low cost fabrication of organic PVs (OPVs) have attracted enormous attention from academy and industry as alternatives to conventional inorganic solar cells.[114–117] Traditionally, OPVs are fabricated on rigid glass substrates coated with indium tin oxide (ITO) as the transparent conductor. In order to take full advantage of OPVs for vehicles and buildings where the surface is usually non-planar,[118] flexible or even stretchable substrates are preferred. However, the brittleness of ITO prevents OPVs from being flexible. Therefore, intensive efforts have been devoted to develop highly conductive and transparent ITO-free electrodes in order to fabricate OPVs on flexible substrates. In this section, we will review the current status of flexible and stretchable OPV devices. Earlier efforts focused on using carbon-based materials, such as carbon nanotubes,[119–122] graphene[123–126] and conducting polymers[127–129] as transparent conductors. The transparency and sheet resistance were recently improved using metal-based nanowires, such as Ag and Cu nanowires.[130–132] From a different application perspective, OPVs with specially designed stretchable electrodes demonstrated robust mechanical properties, while maintaining excellent OPV performance.[133,134]

4.1 Flexible organic solar cells

4.1.1 Carbon-based transparent electrodes. Single walled carbon nanotubes (SWCNTs) have shown great promise in replacing ITO.[119] They have demonstrated potential for use in organic flexible displays,[120] which require high optical transparency and moderate conductivity. A solution processed SWCNT network was investigated as a transparent conductive electrode in polymer-fullerene bulk-hetero-junction solar cells.[121,122] As shown in Fig. 8a–d, the printing method generates relatively smooth and homogenous films with a transmittance of 85% at 550 nm and a sheet resistance of 200 Ω sq^{-1}.[121] The root-mean-square roughness is reduced from 7 nm to 3.5 nm after PEDOT:PSS coating. Fig. 8e demonstrates an efficiency of 2.5% for a PET/SWCNTs/PEDOT:PSS/P3HT:PCBM/Al device structure, compared to the 3% for the ITO based structure. However, due to inter-tube resistance, the conductivity is still limited by a higher sheet resistance, which finally results in a higher series resistance and lower fill factor (FF). Bending tests indicate that the carbon nanotube network is mechanically resilient and there is no efficiency degradation, even at ~5 mm of radii of curvature. In contrast, devices based on ITO on the same 125 μm thick PET substrate begin to fail at a radius of 1 cm. Reducing inter-tube resistance and improving conductivity are essential in the adoption of carbon nanotubes as transparent electrode materials for OPVs.

The increasingly facile production method of graphene film,[123,124] combined with its high conductivity, transparency and mechanical strength, have made it a potential candidate for transparent electrodes. Solution-processing was employed to deposit graphene films with the thickness <20 nm. The graphene film shows >80% transmittance but with a high sheet resistance ranging from 5 kΩ sq^{-1} to 1 MΩ sq^{-1}. As a result, solution-processed graphene-based OPVs show inferior J_{sc} and FF.[125] Chemical-vapor-deposited graphene film gives a much smoother and more homogeneous film and a lower sheet resistance of around 600 Ω sq^{-1} as well as a transmittance of 86% at 550 nm, which indicates that the film quality plays a critical role in sheet resistance. Non-covalently functionalized graphene was also proposed to make hydrophilic surface for the spreading of PEDOT:PSS without losing conductivity. The devices based on graphene modified by pyrene buanoic acid succidymidyl ester (PBASE) exhibit power conversion efficiencies (PCE) of up to 1.71%. In particular, the FF increases from 24.3% to 51.3%. The PBASE incorporation drastically decreases the series resistance of the device, and the PCE of the solar cells made with modified graphene anode can reach 38% of that of a structurally identical cell with an ITO anode.[126] Compared to the 20 Ω sq^{-1} sheet resistance of ITO, graphene's intrinsic boundary resistance of around 1000 Ω sq^{-1} is still large. Conductivity enhancement could be achieved by growing a large area of graphene film and decreasing the film boundary

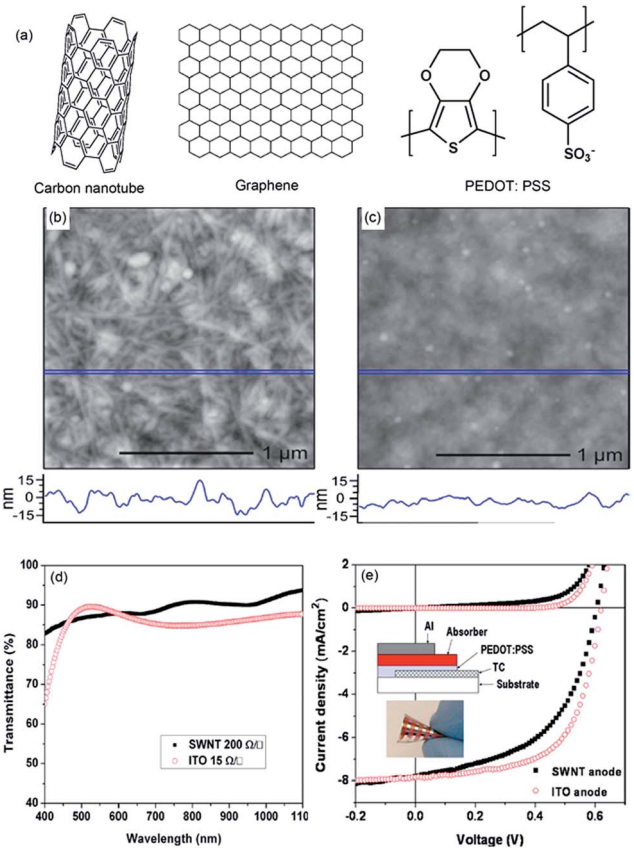

Fig. 8 (a) The structures of SWCNT, graphene, PEDOT:PSS. AFM images of SWCNT network films (b) before and (c) after PEDOT:PSS deposition and annealing at 110 °C for 20 min. (d) Transparency of a 30 nm-thick nanotube film with 200 Ω sq^{-1} sheet resistance, together with the transparency of ITO on glass (15 Ω sq^{-1}). (e) *J*–*V* characteristics of P3HT:PCBM devices under AM1.5G conditions using ITO on glass and flexible SWNTs on PET as the anodes, respectively. Inset: Schematic and photograph of a highly flexible cell using SWNTs on PET. Reprinted from ref. 121.

Published on 16 December 2013. Downloaded by University of Southern California on 06/10/2016 01:42:13.

resistance. Meanwhile, the functionalization of graphene and rigorous optimization should also be done for graphene-based OPVs.

4.1.2 Conducting polymer transparent electrodes. Conducting polymers are promising candidates for flexible transparent electrodes. Considering that carbon nanotubes and graphene-based electrodes still require PEDOT:PSS as an interlayer before depositing the active layer, directly spin-coating PEDOT:PSS on flexible substrates will definitely simplify the fabrication process and pave the way to low cost, lightweight, flexible OPVs. Zhang *et al.* firstly confirmed the feasibility of substituting ITO with a modified PEDOT:PSS as the transparent anode in OPVs.[127] Based on the MEH-PPV/PCBM system, PEDOT:PSS doped with d-sorbitol showed power conversion efficiencies reaching 0.36% compared to 0.46% for an ITO anode. The conductivity of pristine PEDOT:PSS is about 0.006 S cm^{-1}, which is in the insulating regime. In recent years, modified PEDOT:PSS has demonstrated increased conductivity with the addition of inert solvents, such as dimethyl sulfoxide (DMSO), *N*-methylpyrrolidone (NMP), *N*,*N*-dimethylformamide (DMF), ethylene glycol (EG), *etc.* The spin-coated film of PEDOT:PSS doped with 6% EG shows a conductivity of 731 S cm^{-1} and enhanced conductivity of 1418 S cm^{-1} after solvent post treatment. For modified PEDOT:PSS film, a low sheet resistance (<65 Ω sq^{-1}) with a high transparency (>80%) has been achieved.[128] The improvement of conductivity could be attributed to the removal of insulating PSS from the PEDOT:PSS layer.[129]

4.1.3 Metal-based transparent electrodes. The improved conductivity of modified PEDOT:PSS is still much lower than that of ITO. Ag-grids were introduced between the substrate and PEDOT:PSS to increase conductivity and reduce device series resistance.[130–132] The screen-printed Ag grids in combination with highly conductive PEDOT:PSS demonstrated a typical sheet resistance of 1 Ω sq^{-1} with an active area of 4 cm^2. However, the grids account for 6.4–8% of the surface area, which does not contribute to the photocurrent. This shadow effect could be minimized by using metal-based nanostructures, which was reported in both hybrid solar cells and dye-sensitized solar cells.[135,136] Solution processed Ag nanowire mesh was also proposed in OPVs as a transparent electrode alternative to ITO.[137] A slightly higher J_{sc} was obtained compared to that of the device on ITO, benefitting from the scattering effect of random silver nanowires. A comprehensive study on the Ag nanowire electrode shows that the long and thin Ag nanowire is beneficial with respect to sheet resistance and optical transmittance. Both Au coating and mechanical pressing can effectively reduce the junction resistance of Ag nanowires. Ag nanowires also demonstrate outstanding mechanical properties. Compared to the sheet resistance of ITO on polyethylene terephthalate (PET) jumping to 6 kΩ sq^{-1} after being bent, Ag nanowires show little difference, even after being bent to 5 mm 100 times.[138] Meanwhile, Peumans *et al.* showed that a high roughness value of the Ag nanowire electrode could lead to a low shunt resistance with poor device performance. In order to avoid this adverse effect, they demonstrated that by embedding Ag nanowires into the conducting polymer, low roughness Ag nanowires/PEDOT:PSS composite electrodes show an excellent performance of 3.8%, which is better than that of the ITO/PET based structure.[139]

Considering the relatively high cost of silver, electrospun Cu nanofiber webs were developed as less expensive alternatives for transparent electrodes.[140] Fig. 9a shows the schematic and fabrication process of Cu nanofibers. Firstly, $CuAc_2$/PVA composite nanofibers were prepared by electro-spinning. Then the fibers were calcinated in air to form CuO nanofibers. Finally, the CuO nanofibers were reduced to Cu by annealing in an H_2 atmosphere. Fig. 9b shows the current density–voltage (*J*–*V*) curve of the Cu nanofiber-based OPV device with 3% efficiency. Fig. 9c and d shows the much better flexibility of the Cu nanofiber based transparent electrodes than that of the sputtered Cu thin film on PDMS substrate. Furthermore, the Cu nanofiber electrode demonstrated little degradation, while the Cu sputtered film showed an increase of 2 orders in sheet resistance upon stretching to 10% strain. SEM images in Fig. 9e and f also verified that Cu nanofibers still maintained the morphology; whereas the Cu sputtered film broke with some cracks after the bending test. Because calcination and the annealing process were used, a fused junction was formed between Cu nanowires with remarkably reduced junction resistance. Another approach was recently developed by Garnett *et al.*, who used light-induced plasmonic effect to weld Ag nanowires into interconnected networks with significantly reduced junction resistance.[141] Physical parameters and PV

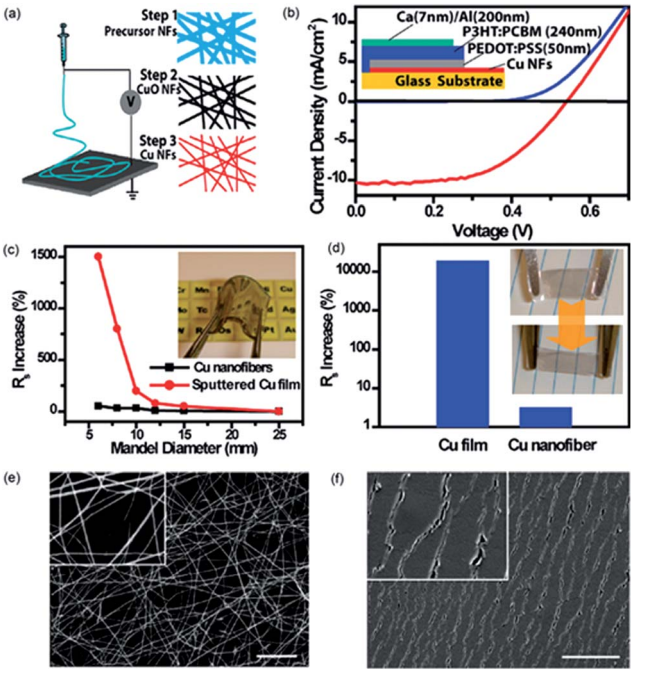

Fig. 9 (a) Schematic of the Cu nanofibers preparation method. Left: schematic of an electro-spinning setup. Right: fabrication process of Cu nanofibers. (b) *J*–*V* curve and device structure (inset) using Cu nanofiber film as the transparent electrode. (c and d) Sheet resistance of Cu nanofibers and sputtered Cu film vary with bending radius and strain. (e and f) SEM images of the Cu nanofiber network and sputtered Cu film after the bending test, scale bar 10 μm. Reprinted from ref. 140.

This journal is © The Royal Society of Chemistry 2014

Published on 16 December 2013. Downloaded by University of Southern California on 06/10/2016 01:42:13.

performance of various types of transparent electrodes on PET substrates are summarized in Table 1.

4.2 Stretchable organic solar cells

Compared to their flexible counterparts, stretchable OPVs have a much more robust mechanical property and can tolerate a range of strain or compression whilst maintaining a superior performance. The compliance of stretchable OPVs allows them to cover moving parts or bond to a curved surface, such as joints in robotic elements and automobiles.[118] The strategy is to exploit the buckling instability that occurs when a compressive strain is applied to a system comprising a rigid film on an elastomeric substrate. Bao's group fabricated the first stretchable OPVs and investigated their mechanical properties.[133] Eutectic gallium indium (EGaIn), a liquid metal alloy, was employed as the top electrode. Conventional top contact-evaporated aluminum cracks catastrophically upon release of the pre-strain. Fig. 10a and b show photographs of a P3HT:PCBM film deposited on pre-strained PDMS substrate and the testing equipment for stretchable OPVs, respectively.

While converting the stretching motions to microscopic bending strain, the peak strain experienced by a thin film under bending strain is directly related to the thickness of the substrate, and inversely related to the radius of curvature, as given by[142]

$$\varepsilon = \left(\frac{d_f + d_s}{2r}\right) \times 100\%$$

where ε is the peak strain, d_f is the thickness of the film, d_s is the thickness of the substrate, and r is the radius of the curvature. In OPVs, the ε and d_f are typically constant. If d_s is reduced, r will decrease correspondingly; that is, the thinner substrate will be much more tolerable towards bending strain.

An ultrathin lightweight OPV stretchable device was fabricated with extreme flexibility.[134] The thickness of the PET substrate was only 1.4 μm and that of the total device was less than 2 μm. As shown in Fig. 10c, the complete device can wrap around a human hair with a radius of 35 μm. When attached to a pre-strained PDMS substrate, the device shows excellent stretchable properties. Fig. 10d shows a stretchable solar cell at various level of compression (left) 0%, (middle) 30%, and (right) 50%. Repeated stretching and compression tests showed a gradual decrease in the J_{sc}, the FF and a marginal loss in power over more than 20 full cycles (Fig. 10f).

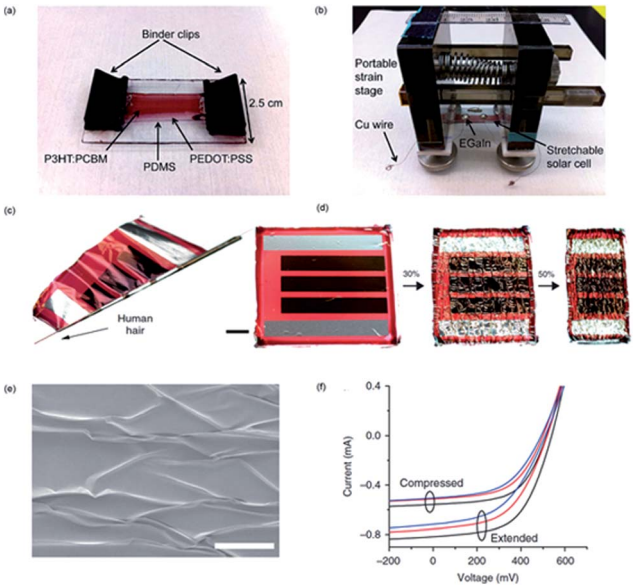

Fig. 10 Photographs of (a) a solar cell on a pre-strained PDMS membrane before deposition of the EGaIn top electrodes, and (b) a purpose-built stage for applying strain to the devices. Reprinted from ref. 133. (c) Extreme bending flexibility demonstrated by wrapping a solar cell around a 35 μm radius human hair. (d) Stretchable solar cells made by attaching the ultrathin solar cell to a pre-stretched elastomer. They are shown 0% (left) and at 30% (middle) and 50% (right) quasi-linear compression. Scale bar (both c and d) 2 mm. (e) SEM image of the PET surface in a compressed state. Scale bar 500 μm. (f) Current–voltage curves at 1 (black), 11 (red) and 22 (blue) cycles for both the fully extended and 50% (quasi-linear) compressed states. Reprinted from ref. 134.

Stretchable OPVs have demonstrated the unique advantage over conventional inorganic solar cells of being highly stretchable. However, better efficiency and longer lifetimes are necessary to make stretchable OPVs more competitive compared to their inorganic counterparts. Much progress has been made in the past few years. By designing various molecular structures to tune electronic energy levels and broaden absorption, chemists have developed systematic strategies to enrich the library of organic photovoltaic materials with significantly improved PCE.[143,144] Improved fabrication and encapsulation technology will further enhance OPV device lifetime. Thus it is very likely that stretchable OPVs with greater efficiency and lifetime will be demonstrated in the near future.

Table 1 Parameters and performance of various transparent electrodes on PET substrate based on the P3HT:PCBM system

Transparent electrode	Transmittance at 550 nm (%)	Sheet resistance (Ω sq^{-1})	V_{OC} (V)	J_{sc}(mA cm^{-2})	FF (%)	PCE (%)	Bending angle/ radius of curvature	Reference
CNT	85	100	0.61	7.8	52	2.5	5 mm	121
Graphene	85	100–1000	0.55	6.1	51	1.7	138°	124 and 126
Ag grids	78	1	0.54	6.3	57	1.9	5 mm	132
Ag nanowires	82	12	0.61	9.7	64	3.8	5 mm	139
Cu nanofibers	90	25	0.55	10.4	53	3.0	6 mm	140
PEDOT:PSS	88	60–176	0.58	11.9	61	4.2	35 μm	129 and 134
ITO	90	20	0.61	10.6	67	4.3	1 cm	116

Published on 16 December 2013. Downloaded by University of Southern California on 06/10/2016 01:42:13.

5 Summary and outlook

This article has reviewed recent progress on flexible solar cells from a number of different aspects, including PV materials, substrate materials, efficient light management, as well as transparent electrodes. As a matter of fact, with the fast evolving of portable and personal electronic devices such as smart phones, embedded sensors, and portable display devices, *etc.*, the lightweight and flexibility of these components/devices has become more important and attractive. In this regard, research on flexible power generation devices, such as solar cells, will receive increasing attention. Meanwhile, flexible PV technologies will not only impact on portable electronics, but also significantly reduce the cost of deployment/installation, which is one of the major components of the cost breakdown of solar panel utilization.

Although crystalline Si PV have been dominating the PV market, thin film PV seems to be advantageous over thick crystalline Si for flexible applications. Nevertheless, it is worth noting that thin crystalline Si and GaAs flexible PV technologies are emerging. These technologies can provide higher power conversion efficiencies as compared to polycrystalline compounds or organic thin film PV, due to high material quality. However, the major bottle neck for their large scale application is the low throughput and high cost fabrication process. Although the competition is fierce, in the near future, the flexible PV applications will still be dominated by a-Si, CIGS, *etc.*

Acknowledgements

Q. L., H. F. and Z. F. acknowledge the support by ITS/192/11 from the Hong Kong Innovation Technology Commission and General Research Fund (612111) from Hong Kong Research Grant Council. H.H. and D. L. are thankful for the financial support from the Science & Technology Commission of the Shanghai Municipality (Grant no. 13DZ1106000), the National Natural Science Foundation of China (Grant no. 51102271), the Natural Science Foundation of Shanghai (Grant no. 11ZR1436300), the Korea Institute of Industrial Technology through the Korea-China Cooperative R&D Program. (Granted no: JE130001) and the New & Renewable Energy Technology Development Program of the Korea Institute of Energy Technology Evaluation and Planning(KETEP) grant funded by the Korea government Ministry of Trade, Industry & Energy. (no. 20113020010010). Y. Y. acknowledge the support from UH start-up fund, the Ralph E. Powe Junior Faculty Enhancement Award from ORAU, and the TcSUH Welch Foundation Professorship Award (E-0001). Y. J. is grateful for the UH presidential fellowship.

Notes and references

1 IEA, *Key World Energy Statistics*, Paris, 2012.
2 J. Weickert, R. B. Dunbar, H. C. Hesse, W. Wiedemann and L. Schmidt-Mende, *Adv. Mater.*, 2011, **23**, 1810.
3 M. Pagliaro, R. Ciriminna and G. Palmisano, *ChemSusChem*, 2008, **1**, 880.
4 OECD/IEA, *World Energy Outlook*, London, 2012.
5 N. S. Lewis, *Science*, 2007, **315**, 798.
6 J. Perlin, *From Space to Earth: The Story of Solar Electricity*, Earthscan, 1999.
7 M. B. Schubert and J. H. Werner, *Mater. Today*, 2006, **9**, 42.
8 J. Yang, A. Banerjee and S. Guha, *Appl. Phys. Lett.*, 1997, **70**, 2975.
9 Z. Fan and A. Javey, *Nat. Mater.*, 2008, **7**, 835.
10 R. M. Swanson, *Progr. Photovolt.: Res. Appl.*, 2006, **14**, 443.
11 J. Zhao, A. Wang and M. A. Green, *Progr. Photovolt.: Res. Appl.*, 1999, **7**, 144.
12 A. Wang, J. Zhao, S. Wenham and M. Green, *Progr. Photovolt.: Res. Appl.*, 1996, **4**, 55.
13 M. A. Green, *IEEE Trans. Electron Devices*, 1984, **31**, 671.
14 G. Willeke, *Sol. Energy Mater. Sol. Cells*, 2002, **72**, 191.
15 T. Yonehara, K. Sakaguchi and N. Sato, *Appl. Phys. Lett.*, 1994, **64**, 2108.
16 K. Weber, K. Catchpole and A. Blakers, *J. Cryst. Growth*, 1998, **186**, 369.
17 R. Bilyalov, L. Stalmans, G. Beaucarne, R. Loo, M. Caymax, J. Poortmans and J. Nijs, *Sol. Energy Mater. Sol. Cells*, 2001, **65**, 477.
18 X. Zhang, S. Collins and R. Smith, *J. Electrochem. Soc.*, 1989, **136**, 1561.
19 C. Solanki, R. Bilyalov, J. Poortmans, J. Nijs and R. Mertens, *Sol. Energy Mater. Sol. Cells*, 2004, **83**, 101.
20 C. Berge, M. Zhu, W. Brendle, M. Schubert and J. Werner, *Sol. Energy Mater. Sol. Cells*, 2006, **90**, 3102.
21 NREL, http://www.nrel.gov/ncpv/images/efficiency_chart.jpg, 2013.
22 J. Yoon, A. J. Baca, S. I. Park, P. Elvikis, J. B. Geddes, L. Li, R. H. Kim, J. Xiao, S. Wang, T. H. Kim, M. J. Motala, B. Y. Ahn, E. B. Duoss, J. A. Lewis, R. G. Nuzzo, P. M. Ferreir, Y. Huang, A. Rockett and J. A. Rogers, *Nat. Mater.*, 2008, **7**, 907.
23 J. L. Cruz-Campa, M. Okandan, P. J. Resnick, P. Clews, T. Pluym, R. K. Grubbs, V. P. Gupta, D. Zubia and G. N. Nielson, *Sol. Energy Mater. Sol. Cells*, 2011, **95**, 551.
24 S. W. Bedell, D. Shahrjerdi, B. Hekmatshoar, K. Fogel, P. A. Lauro, J. A. Ott, N. Sosa and D. Sadana, *IEEE J. Photovoltaics*, 2012, **2**, 141.
25 R. Rao, L. Mathew, S. Saha, S. Smith, D. Sarkar, R. Garcia, R. Stout, A. Gurmu, E. Onyegam and D. Ahn, *37th IEEE PVSC*, 2011, p. 001504.
26 S. Saha, M. M. Hilali, E. U. Onyegam, D. Sarkar, D. Jawarani, R. A. Rao, L. Mathew, R. S. Smith, D. Xu and U. K. Das, *Appl. Phys. Lett.*, 2013, **102**, 163904.
27 A. Mahan, J. Carapella, B. Nelson, R. Crandall and I. Balberg, *J. Appl. Phys.*, 1991, **69**, 6728.
28 M. Goto, H. Toyoda, M. Kitagawa, T. Hirao and H. Sugai, *Jpn. J. Appl. Phys.*, 1997, **36**, 3714.
29 A. Shah, J. Dutta, N. Wyrsch, K. Prasad, H. Curtins, F. Finger, A. Howling and C. Hollenstein, *MRS Online Proc. LIbr.*, 1992, **258**, 15.

 This journal is © The Royal Society of Chemistry 2014

Published on 16 December 2013. Downloaded by University of Southern California on 06/10/2016 01:42:13.

30 R. Collins, A. Ferlauto, G. Ferreira, C. Chen, J. Koh, R. Koval, Y. Lee, J. Pearce and C. Wronski, *Sol. Energy Mater. Sol. Cells*, 2003, **78**, 143.
31 M. Izu and T. Ellison, *Sol. Energy Mater. Sol. Cells*, 2003, **78**, 613.
32 Y. Ichikawa, T. Yoshida, T. Hama, H. Sakai and K. Harashima, *Sol. Energy Mater. Sol. Cells*, 2001, **66**, 107.
33 Y. Ichikawa, S. Fujikake, H. Ohta, T. Sasaki and H. Sakai, *22nd IEEE PVSC*, 1991, p. 1296.
34 S. Guha and J. Yang, *IEEE Trans. Electron Devices*, 1999, **46**, 2080.
35 S. Guha, J. Yang, A. Pawlikiewicz, T. Glatfelter, R. Ross and S. Ovshinsky, *Appl. Phys. Lett.*, 1989, **54**, 2330.
36 J. Woerdenweber, T. Merdzhanova, T. Zimmermann, A. Flikweert, H. Stiebig, W. Beyer and A. Gordijn, *J. Non-Cryst. Solids*, 2012, **358**, 2183.
37 A. Shah, H. Schade, M. Vanecek, J. Meier, E. Vallat-Sauvain, N. Wyrsch, U. Kroll, C. Droz and J. Bailat, *Progr. Photovolt.: Res. Appl.*, 2004, **12**, 113.
38 X. Xu, T. Su, S. Ehlert, G. Pietka, D. Bobela, D. Beglau, J. Zhang, Y. Li, G. DeMaggio and C. Worrel, *35th IEEE PVSC*, 2010, p. 001141.
39 Q. H. Fan, M. Deng, X. Liao and X. Deng, *J. Appl. Phys.*, 2009, **105**, 033304.
40 S. Hegedus, *Progr. Photovolt.: Res. Appl.*, 2006, **14**, 393.
41 A. Yusoff, M. Syahrul and K. Henkel, *Bull. Mater. Sci.*, 2007, **30**, 329.
42 F. Liu, K. Beernink, C. Hu, X. Xu, A. Banerjee, G. DeMaggio, G. Pietka, J. Yang and S. Guha, *33rd IEEE PVSC*, 2008, p. 1.
43 X. Xu, K. Lord, G. Pietka, F. Liu, K. Beernink, B. Yan, C. Worrel, G. DeMaggio, A. Banerjee and J. Yang, *33rd IEEE PVSC*, 2008, p. 1.
44 A. Banerjee, X. Xu, K. Beernink, F. Liu, K. Lord, G. DeMaggio, B. Yan, T. Su, G. Pietka and C. Worrel, *35th IEEE PVSC*, 2010, p. 002651.
45 C. H. Lee, D. R. Kim, I. S. Cho, N. William, Q. Wang and X. Zheng, *Sci. Rep.*, 2012, **2**, 1000.
46 Q. Lin, B. Hua, S. Leung, X. Duan and Z. Fan, *ACS Nano*, 2013, **7**, 2725.
47 K. X. Wang, Z. Yu, V. Liu, Y. Cui and S. Fan, *Nano Lett.*, 2012, **12**, 1616.
48 R. Yu, Q. Lin, S. F. Leung and Z. Fan, *Nano Energy*, 2012, **1**, 57.
49 B. Hua, Q. Lin, Q. Zhang and Z. Fan, *Nanoscale*, 2013, **5**, 6627.
50 Z. Y. Fan, R. Kapadia, P. W. Leu, X. B. Zhang, Y. L. Chueh, K. Takei, K. Yu, A. Jamshidi, A. A. Rathore, D. J. Ruebusch, M. Wu and A. Javey, *Nano Lett.*, 2010, **10**, 3823.
51 S. F. Leung, M. Yu, Q. Lin, K. Kwon, K. L. Ching, L. Gu, K. Yu and Z. Fan, *Nano Lett.*, 2012, **12**, 3682.
52 R. Yu, K. Ching, Q. Lin, S. Leung, D. Arcrossito and Z. Fan, *ACS Nano*, 2011, **5**, 9291.
53 S. Wang, B. D. Weil, Y. Li, K. X. Wang, E. Garnett, S. Fan and Y. Cui, *Nano Lett.*, 2013, **13**, 4393.
54 H. Huang, L. Lu, J. Wang, J. Yang, S. Leung, Y. Wang, D. Chen, X. Chen, G. Shen and D. D. Li, *Energy Environ. Sci.*, 2013, **6**, 2965.
55 M. H. Lee, N. Lim, D. J. Ruebusch, A. Jamshidi, R. Kapadia, R. Lee, T. J. Seok, K. Takei, K. Y. Cho, Z. Y. Fan, H. Jang, M. Wu, G. J. Cho and A. Javey, *Nano Lett.*, 2011, **11**, 3425.
56 A. Chirilă, S. Buecheler, F. Pianezzi, P. Bloesch, C. Gretener, A. R. Uhl, C. Fella, L. Kranz, J. Perrenoud and S. Seyrling, *Nat. Mater.*, 2011, **10**, 857.
57 L. Kranz, C. Gretener, J. Perrenoud, R. Schmitt, F. Pianezzi, F. La Mattina, P. Blösch, E. Cheah, A. Chirilă and C. M. Fella, *Nat. Commun.*, 2013, **4**, 2306.
58 J. Lee, J. Wu, M. Shi, J. Yoon, S. Park, M. Li, Z. Liu, Y. Huang and J. A. Rogers, *Adv. Mater.*, 2011, **23**, 986.
59 J. Lee, J. Wu, J. H. Ryu, Z. Liu, M. Meitl, Y. Zhang, Y. Huang and J. A. Rogers, *Small*, 2012, **8**, 1851.
60 H. Katagiri, K. Jimbo, W. S. Maw, K. Oishi, M. Yamazaki, H. Araki and A. Takeuchi, *Thin Solid Films*, 2009, **517**, 2455.
61 Q. Guo, G. M. Ford, W. Yang, B. C. Walker, E. A. Stach, H. W. Hillhouse and R. Agrawal, *J. Am. Chem. Soc.*, 2010, **132**, 17384.
62 P. K. Sarswat, M. Snure, M. L. Free and A. Tiwari, *Thin Solid Films*, 2012, **520**, 1694.
63 H. Katagiri, *3rd IEEE ICP*, 2012, p. 345.
64 V. P. Singh, J. C. McClure, G. Lush, W. Wang, X. Wang, G. Thompson and E. Clark, *Sol. Energy Mater. Sol. Cells*, 1999, **59**, 145.
65 I. Matulionis, S. Han, J. A. Drayton, K. J. Price and A. D. Compaan, *MRS Proceedings*, 2001, **668**(H8), 23.
66 D. Shen, V. Palekis, D. Hodges, S. Bhandaru, V. Guntur, E. Stefanakos, D. Morel and C. Ferekides, *35th IEEE PVSC*, 2010, p. 001973.
67 X. Feng, K. Singh, S. Bhavanam, V. Palekis, D. L. Morel and C. S. Ferekides, *38th IEEE PVSC*, 2012, p. 000843.
68 X. Feng, K. Singh, S. Bhavanam, V. Palekis, D. L. Morel and C. Ferekides, *Thin Solid Films*, 2012, **535**, 202.
69 V. P. Singh and J. C. McClure, *Sol. Energy Mater. Sol. Cells*, 2003, **76**, 369.
70 J. P. Enríquez, X. Mathew, G. Hernández, U. Pal, C. Magana, D. Acosta, R. Guardian, J. Toledo, G. Contreras Puente and J. Chávez Carvayar, *Sol. Energy Mater. Sol. Cells*, 2004, **82**, 307.
71 J. Drayton, A. Vasko, A. Gupta and A. Compaan, *31st IEEE PVSC*, 2005, p. 406.
72 A. Tiwari, A. Romeo, D. Baetzner and H. Zogg, *Progr. Photovolt.: Res. Appl.*, 2001, **9**, 211.
73 A. Romeo, M. Arnold, D. Bätzner, H. Zogg and A. Tiwari, *PV in Europe – from PV Technology to Energy Solutions*, 2002, p. 377.
74 A. Romeo, G. Khrypunov, F. Kurdesau, M. Arnold, D. Bätzner, H. Zogg and A. Tiwari, *Sol. Energy Mater. Sol. Cells*, 2006, **90**, 3407.
75 J. Perrenoud, S. Buecheler and A. Tiwari, *Proc. SPIE 7409, Thin Film Solar Technology*, 2009, p. 74090L.
76 EMPA, www.empa.ch/plugin/template/empa/*/110807, 2011.
77 B. Basol, V. Kapur, A. Halani and C. Leidholm, *Sol. Energy Mater. Sol. Cells*, 1993, **29**, 163.

Published on 16 December 2013. Downloaded by University of Southern California on 06/10/2016 01:42:13.

78 M. Hartmann, M. Schmidt, A. Jasenek, H. W. Schock, F. Kessler, K. Herz and M. Powalla, *28th IEEE PVSC*, 2000, p. 638.
79 S. Ishizuka, A. Yamada, K. Matsubara, P. Fons, K. Sakurai and S. Niki, *Appl. Phys. Lett.*, 2008, **93**, 124105.
80 M. A. Contreras, B. Egaas, K. Ramanathan, J. Hiltner, A. Swartzlander, F. Hasoon and R. Noufi, *Progr. Photovolt.: Res. Appl.*, 1999, **7**, 311.
81 R. Wuerz, A. Eicke, F. Kessler, S. Paetel, S. Efimenko and C. Schlegel, *Sol. Energy Mater. Sol. Cells*, 2012, **100**, 132.
82 B. M. Başol, V. K. Kapur, C. R. Leidholm, A. Halani and K. Gledhill, *Sol. Energy Mater. Sol. Cells*, 1996, **43**, 93.
83 A. Tiwari, M. Krejci, F. Haug and H. Zogg, *Progr. Photovolt.: Res. Appl.*, 1999, **7**, 393.
84 M. Faraj, K. Ibrahim and A. Salhin, *Int. J. Polym. Mater.*, 2011, **60**, 817.
85 S. Niki, M. Contreras, I. Repins, M. Powalla, K. Kushiya, S. Ishizuka and K. Matsubara, *Prog. Photovoltaics*, 2010, **18**, 453.
86 A. Neisser, C. Kaufmann, M. Kroon, R. Klenk and R. Scheer, *IEEE 3rd World Conference on Photovoltaic Energy Conversion*, 2003, vol. 1, p. 458.
87 C. A. Kaufmann, A. Neisser, R. Klenk, R. Scheer and H. W. Schock, *MRS Online Proc. LIbr.*, 2005, **865**, F7-5.
88 T. Yagioka, *Appl. Phys. Express*, 2009, **2**, 2201.
89 S. Ishizuka, A. Yamada and S. Niki, *34th IEEE PVSC*, 2009, p. 002349.
90 F. Pianezzi, A. Chirilă, P. Blösch, S. Seyrling, S. Buecheler, L. Kranz, C. Fella and A. Tiwari, *Prog. Photovoltaics*, 2012, **20**, 253.
91 D. Brémaud, D. Rudmann, G. Bilger, H. Zogg and A. Tiwari, *31st IEEE PVSC*, 2005, p. 223.
92 P. Reinhard, A. Chirila, P. Blosch, F. Pianezzi, S. Nishiwaki, S. Buecheler and A. N. Tiwari, *IEEE J. Photovoltaics*, 2013, **3**, 572.
93 A. Chirilă, P. Bloesch, S. Seyrling, A. Uhl, S. Buecheler, F. Pianezzi, C. Fella, J. Perrenoud, L. Kranz and R. Verma, *Prog. Photovoltaics*, 2011, **19**, 560.
94 S. Ishizuka, T. Yoshiyama, K. Mizukoshi, A. Yamada and S. Niki, *Sol. Energy Mater. Sol. Cells*, 2010, **94**, 2052.
95 P. Jackson, D. Hariskos, E. Lotter, S. Paetel, R. Wuerz, R. Menner, W. Wischmann and M. Powalla, *Prog. Photovoltaics*, 2011, **19**, 894.
96 K. Bertness, S. R. Kurtz, D. Friedman, A. Kibbler, C. Kramer and J. Olson, *Appl. Phys. Lett.*, 1994, **65**, 989.
97 E. Yablonovitch, T. Gmitter, J. P. Harbison and R. Bhat, *Appl. Phys. Lett.*, 1987, **51**, 2222.
98 J. Schermer, P. Mulder, G. Bauhuis, M. Voncken, J. Van Deelen, E. Haverkamp and P. Larsen, *Phys. Status Solidi A*, 2005, **202**, 501.
99 R. Tatavarti, G. Hillier, G. Martin, A. Wibowo, R. Navaratnarajah, F. Tuminello, D. Hertkorn, M. Disabb, C. Youtsey and D. McCallum, *34th IEEE PVSC*, 2009, p. 002065.
100 G. Bauhuis, P. Mulder, E. Haverkamp, J. Huijben and J. Schermer, *Sol. Energy Mater. Sol. Cells*, 2009, **93**, 1488.
101 B. M. Kayes, H. Nie, R. Twist, S. G. Spruytte, F. Reinhardt, I. C. Kizilyalli and G. S. Higashi, *37th IEEE PVSC*, 2011, p. 000004.
102 M. W. Wanlass, S. Ahrenkiel, R. Ahrenkiel, D. Albin, J. Carapella, A. Duda, J. Geisz, S. Kurtz, T. Moriarty and R. Wehrer, *31st IEEE PVSC*, 2005, p. 530.
103 T. Takamoto, T. Agui, A. Yoshida, K. Nakaido, H. Juso, K. Sasaki, K. Nakamora, H. Yamaguchi, T. Kodama and H. Washio, *35th IEEE PVSC*, 2010, p. 000412.
104 T. Takamoto, T. Agui, H. Washio, N. Takahashi, K. Nakamura, O. Anzawa, M. Kaneiwa, K. Kamimura, K. Okamoto and M. Yamaguchi, *31st IEEE PVSC*, 2005, p. 519.
105 T. Takamoto, M. Kaneiwa, M. Imaizumi and M. Yamaguchi, *Progr. Photovolt.: Res. Appl.*, 2005, **13**, 495.
106 T. Takamoto, T. Kodama, H. Yamaguchi, T. Agui, N. Takahashi, H. Washio, T. Hisamatsu, M. Kaneiwa, K. Okamoto and M. Imaizumi, *IEEE 4th World Conference on Photovoltaic Energy Conversion*, 2006, vol. 2, p. 1769.
107 D. C. Law, K. Edmondson, N. Siddiqi, A. Paredes, R. King, G. Glenn, E. Labios, M. Haddad, T. Isshiki and N. Karam, *IEEE 4th World Conference on Photovoltaic Energy Conversion*, 2006, vol. 2, p. 1879.
108 C. Morioka, K. Shimazaki, S. Kawakita, M. Imaizumi, H. Yamaguchi, T. Takamoto, S. Sato, T. Ohshima, Y. Nakamura and K. Hirako, *Prog. Photovoltaics*, 2011, **19**, 825.
109 L. S. Mattos, S. R. Scully, M. Syfu, E. Olson, L. Yang, C. Ling, B. M. Kayes and G. He, *38th IEEE PVSC*, 2012, p. 003187.
110 K. M. Edmondson, D. Law, G. Glenn, A. Paredes, R. King and N. Karam, *IEEE 4th World Conference on Photovoltaic Energy Conversion*, 2006, vol. 2, p. 1935.
111 J. Yoon, S. Jo, I. S. Chun, I. Jung, H. Kim, M. Meitl, E. Menard, X. Li, J. J. Coleman and U. Paik, *Nature*, 2010, **465**, 329.
112 C. Youtsey, J. Adams, R. Chan, V. Elarde, G. Hillier, M. Osowski, D. McCallum, H. Miyamoto, N. Pan and C. Stender, *CS MANTECH Conference*, 2012.
113 D. Shahrjerdi, S. W. Bedell, C. Bayram, C. C. Lubguban, K. Fogel, P. Lauro, J. A. Ott, M. Hopstaken, M. Gayness and D. Sadana, *Adv. Energy Mater.*, 2013, **3**, 566.
114 S. R. Forrest, *Nature*, 2004, **428**, 911.
115 C. J. Brabec, N. S. Sariciftci and J. C. Hummelen, *Adv. Funct. Mater.*, 2001, **11**, 15.
116 G. Li, V. Shrotriya, J. S. Huang, Y. Yao, T. Moriarty, K. Emery and Y. Yang, *Nat. Mater.*, 2005, **4**, 864.
117 G. Li, R. Zhu and Y. Yang, *Nat. Photonics*, 2012, **6**, 153.
118 D. J. Lipomi and Z. Bao, *Energy Environ. Sci.*, 2011, **4**, 3314.
119 D. Zhang, K. Ryu, X. Liu, E. Polikarpov, J. Ly, M. E. Tompson and C. Zhou, *Nano Lett.*, 2006, **6**, 1880.
120 W. Choi, D. Chung, J. Kang, H. Kim, Y. Jin, I. Han, Y. Lee, J. Jung, N. Lee and G. Park, *Appl. Phys. Lett.*, 1999, **75**, 3129.
121 M. W. Rowell, M. A. Topinka, M. D. McGehee, H. Prall, G. Dennler, N. S. Sariciftci, L. Hu and G. Gruner, *Appl. Phys. Lett.*, 2006, **88**, 233506.
122 J. Van De Lagemaat, T. M. Barnes, G. Rumbles, S. E. Shaheen, T. J. Coutts, C. Weeks, I. Levitsky, J. Peltola and P. Glatkowski, *Appl. Phys. Lett.*, 2006, **88**, 233503.

 This journal is © The Royal Society of Chemistry 2014

Published on 16 December 2013. Downloaded by University of Southern California on 06/10/2016 01:42:13.

123 K. S. Kim, Y. Zhao, H. Jang, S. Y. Lee, J. M. Kim, K. S. Kim, J. Ahn, P. Kim, J. Choi and B. H. Hong, *Nature*, 2009, **457**, 706.
124 S. Pang, Y. Hernandez, X. Feng and K. Müllen, *Adv. Mater.*, 2011, **23**, 2779.
125 J. Wu, H. A. Becerril, Z. Bao, Z. Liu, Y. Chen and P. Peumans, *Appl. Phys. Lett.*, 2008, **92**, 263302.
126 Y. Wang, X. Chen, Y. Zhong, F. Zhu and K. P. Loh, *Appl. Phys. Lett.*, 2009, **95**, 063302.
127 F. Zhang, M. Johansson, M. R. Andersson, J. C. Hummelen and O. Inganäs, *Adv. Mater.*, 2002, **14**, 662.
128 S. Na, S. Kim, J. Jo and D. Kim, *Adv. Mater.*, 2008, **20**, 4061.
129 Y. H. Kim, C. Sachse, M. L. Machala, C. May, L. Müller-Meskamp and K. Leo, *Adv. Funct. Mater.*, 2011, **21**, 1076.
130 T. Aernouts, P. Vanlaeke, W. Geens, J. Poortmans, P. Heremans, S. Borghs, R. Mertens, R. Andriessen and L. Leenders, *Thin Solid Films*, 2004, **451**, 22.
131 K. Tvingstedt and O. Inganäs, *Adv. Mater.*, 2007, **19**, 2893.
132 Y. Galagan, J. J. M. Rubingh, R. Andriessen, C. Fan, P. W. M. Blom, S. C. Veenstra and J. M. Kroon, *Sol. Energy Mater. Sol. Cells*, 2011, **95**, 1339.
133 D. J. Lipomi, B. C. Tee, M. Vosgueritchian and Z. Bao, *Adv. Mater.*, 2011, **23**, 1771.
134 M. Kaltenbrunner, M. S. White, E. D. Głowacki, T. Sekitani, T. Someya, N. S. Sariciftci and S. Bauer, *Nat. Commun.*, 2012, **3**, 770.
135 W. U. Huynh, J. J. Dittmer and A. P. Alivisatos, *Science*, 2002, **295**, 2425.
136 S. Chu, D. Li, P. Chang and J. G. Lu, *Nanoscale Res. Lett.*, 2011, **6**, 38.
137 J. Lee, S. T. Connor, Y. Cui and P. Peumans, *Nano Lett.*, 2008, **8**, 689.
138 L. Hu, H. S. Kim, J. Lee, P. Peumans and Y. Cui, *ACS Nano*, 2010, **4**, 2955.
139 W. Gaynor, G. F. Burkhard, M. D. McGehee and P. Peumans, *Adv. Mater.*, 2011, **23**, 2905.
140 H. Wu, L. Hu, M. W. Rowell, D. Kong, J. J. Cha, J. R. McDonough, J. Zhu, Y. Yang, M. D. McGehee and Y. Cui, *Nano Lett.*, 2010, **10**, 4242.
141 E. C. Garnett, W. Cai, J. J. Cha, F. Mahmood, S. T. Connor, M. G. Christoforo, Y. Cui, M. D. McGehee and M. L. Brongersma, *Nat. Mater.*, 2012, **11**, 241.
142 Z. Suo, E. Ma, H. Gleskova and S. Wagner, *Appl. Phys. Lett.*, 1999, **74**, 1177.
143 Y. Li, *Acc. Chem. Res.*, 2012, **45**, 723.
144 L. Huo and J. Hou, *Polym. Chem.*, 2011, **2**, 2453.